Digest Journal of Nanomaterials and Biostructures Vol. 12, No. 3, July - September 2017, p. 631 - 637

FACILE SYNTHESIS AND PHOTOLUMINESCENCE PROPERTIES OF NOVEL HEPARIN/$CaMoO_4$: Yb, Er BIOCOMPOSITES

Y. GAO[a,b*], Q. WU[a], X. LIN[a], X. ZHANG[a]
[a]*College of Ocean, Hainan University, Haikou 570228, China*
[b]*Key Laboratory of Tropical Biological Resources of Ministry of Education, Hainan University, Haikou 570228, China*

Novel heparin/$CaMoO_4$: Yb, Er biocomposites (heparin/$CaMoO_4$) are synthesized by a facile hydrothermal routes with Na_2EDTA as a chelating agent. XRD, SEM, and photoluminescence (PL) spectra have been used to characterize the size, morphology and photoluminescence spectrum of the heparin/$CaMoO_4$. Heparin and $CaMoO_4$ nanoparticles are shaped into a homogeneous biocomposites. The latent photoinduced electrons transfer between heparin and $CaMoO_4$ nanocrystals weaken upconversion (UC) luminescence intensity of heparin/$CaMoO_4$, but the aqueous dispersion of heparin/$CaMoO_4$ still present naked eye-visible greem luminescence under a 980 nm laser in the power density only about 50 $mWcm^{-2}$. Obtained heparin/$CaMoO_4$ biocomposites will paves the way for promising applications in biomedical fields as luminescent bioprobes.

(Received March 27, 2017; Accepted July 1, 2017)

Keywords: heparin; $CaMoO_4$; biocomposites; chemical synthesis; photoluminescence

1. Introduction

Heparin is a linear polysaccharide which consists of 1-4 linked disaccharide repeating units of uronic acid and glucosamine residues. Heparin plays an important role in many biocomposites via its interaction with various proteins, and hydrogels and nanoparticles comprising heparin exhibit attractive properties, such as anticoagulant activity, growth factor binding, and antiangiogenic and apoptotic effects, making them great candidates for emerging applications.[1] Many kinds of functional nanoparticles, such as Au, Fe_3O_4, and SiO_2 nanoparticles have been successfully combined with heparin or its derivatives.[2-4] The emergence of novel biocompatible luminescent probes and multiphoton fluorescence microscopy has had a significant impact on imaging cells, both in vivo and in vitro.[5] However, studies on the biocomposites of UC luminescent nanocrystals and heparin, which generates superior luminescence and well biocompatible performance by combining the advantages of both, are still few.

Recently, lanthanide doped upconversion nanoparticles (UPNP) such as, $NaYF_4$: Yb, Er, $CaMoO_4$: Yb, Er, represent a new generation of luminescent probes.[6, 7] These nanoparticles have a unique ability to upconvert near-infrared radiation (NIR), to visible or ultraviolet light.[5, 8] Other distinct advantages, such as minimal background autofluorescence and photobleaching under near infrared (NIR) excitation, high room-temperature quantum yields and long luminescence life time result in a fact that Ln^{3+}-doped UPNP are regarded as an ideal fluorescence labeling material for potential applications in many fields, especially in biomedicine.[9] The functionalization of these nanoparticles with naturally occurring polysaccharides, which play an important role in protein and cell interactions, tissue regeneration, drug delivery, cancer diagnosis and treatment, may provide a considerable potential in a variety of bioimaging applications.[4, 10] Therefore, it's very necessary to develop a facile way for the biocomposites of UPNP and heparin with good luminescence intensity and excellent biocompatibility.

* Corresponding author: gaoyong_1997@sina.com

In this work we report on the very straightforward synthesis of advanced biocompatible imaging nanoprobes, heparin/$CaMoO_4$. Our design involves a continuous process. In the 90 °C water, a stoichiometric amount of rare earth compound solution, Na_2EDTA solution, and $(NH_4)_6Mo_7O_{24}$ solution are mixed one by one. A half hour later, the mixture is mixed with heparin sodium solution, and the hydrothermal process at 180 °C is carried out. The morphology and microstructure of heparin/$CaMoO_4$ were investigated by X-ray powder diffraction (XRD) and scanning electron microscopy (SEM). The influence of adding quantity of heparin for the UC luminescence of heparin/$CaMoO_4$ is investigated. The possible energy transfer from the UPNS to the energy receptor in heparin substrate is also explored.

2. Experimental and Characterization

2.1 Synthesis of heparin/$CaMoO_4$ nanocomposite

All chemicals were used directly without further purification. In a typical procedure, 16 ml of 0.1M $Ca(NO_3)_2$, 3.6 ml of 0.1M $Yb(NO_3)_3$, and 0.4 ml of 0.1M $Er(NO_3)_2$ were prepared in a beaker with 90 °C distilled water by constant stirring with magnetic stirrer. And then 25 ml of 0.1 M Na_2EDTA solution was added into previous mixture. In a separate beaker, 20 mM $(NH_4)_6Mo_7O_{24}$ was prepared in 95 °C distilled water. After that, $(NH_4)_6Mo_7O_{24}$ solution was added into previous mixture under continuous stirring. The pH of the resulting solution was adjusted by aqueous ammonia solution. A half hour later, the mixture are mixed with heparin sodium solution (1.5 wt%). A half hour later, the mixture was transferred to Teflon-lined autoclave and heated at 180 °C for 2 h. Obtained sample were purified by centrifugation, washed with DI water and dried under vacuum.

2.2 Characterization

XRD measurements were performed on a Bruker D8 Advance X-ray diffractometer with Cu Kα (λ = 1.5418 Å) radiation. The SEM micrographs were obtained using scanning electron microscopy (SEM, S-3000N, Hitachi). The Transmission electron microscopy (TEM) and high-resolution transmission electron microscopy (HRTEM) were characterized by a JEOL 2100 running at an accelerating voltage of 200 kV. Fourier-transform infrared spectrometry (FT-IR) was recorded on a Bruker TENSOR27 IR spectrophotometer, and the sample were pulverized with KBr and pressed into pellets. The thermo-gravimetric analysis (TGA) was carried out with a SDT Q600 analyzer with a heating rate of 10˚C min^{-1}, and the sample was measured in a corundum crucible in nitrogen atmosphere from room temperature to 510 ˚C. The photoluminescence spectra were recorded using an F-7000 spectrofluorimeter (Hitachi, Japan) with an external 980 nm laser as the excitation source.

3. Results and discussion

To obtain the structure information about as-prepared heparin/$CaMoO_4$ biocomposites, powder XRD characterization is conducted. For comparing and analyzing the influence of heparin, $CaMoO_4$:Yb,Er nanocrystals without heparin are prepared by a hydrothermal route. As shown in Fig. 1, the peak positions and intensities of $CaMoO_4$:Yb,Er nanocrystals without heparin agree well with the data reported in the JCPDS standard card (77-2240) of pure tetragonal $CaMoO_4$ crystals.[11] For obtained heparin/$CaMoO_4$ biocomposites, it is clear that heparin/$CaMoO_4$ biocomposites contains XRD signals of both heparin and a standard sample of $CaMoO_4$ crystals, which indicating that biocomposites retains the crystal structures of both material. Several strong diffraction peaks in the XRD patterns observed at 2θ = 18.5°, 29.1°, 31.5°, 34.6°, and 58.6°, can be assigned to the (101), (112), (004), (200), and (312) reflections of $CaMoO_4$:Yb,Er nanoparticles, respectively. [11] Also, a weaker characteristic peak of heparin located at about 23° in the XRD patterns of heparin/$CaMoO_4$ reveal that $CaMoO_4$:Yb,Er nanoparticles attached with heparin sheets destroy the nature orientation of heparin [12].

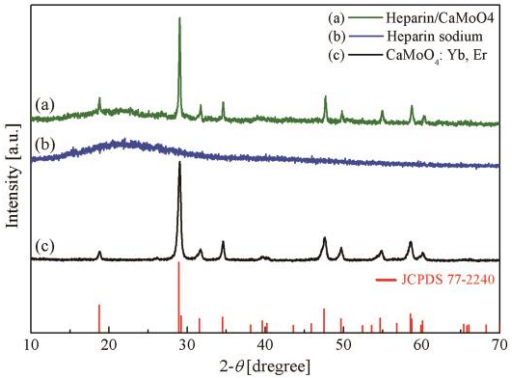

Fig 1. XRD patterns of as-prepared $CaMoO_4$:Yb,Er nanocrystals, heparin/$CaMoO_4$ biocomposites, and heparin sodium [red vertical bars at the bottom are standard tetragonal phase $CaMoO_4$ crystal (JCPDS 77-2240)].

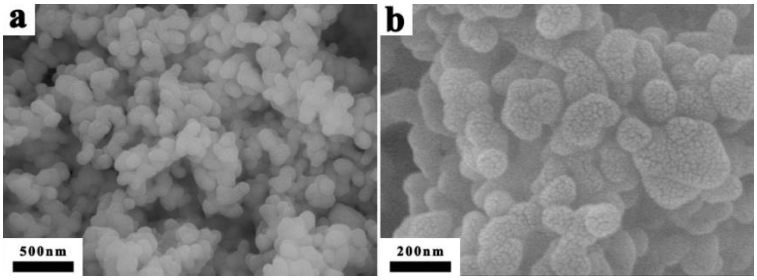

Fig 2. SEM images of obtained heparin/$CaMoO_4$ biocomposites.

SEM images show the direct morphology of obtained heparin/$CaMoO_4$ biocomposites. As shown in Fig. 2, heparin and $CaMoO_4$:Yb, Er nanocrystals have been constructed to be a homogeneous biocomposites, and the biocomposites are spherical in shape with a mean diameter of approximately 150 nm. Also, the particles are reasonably uniform in size. Higher magnification SEM image (Fig. 2 b) shows the surface of heparin/$CaMoO_4$ is unsmooth. And the heparin/$CaMoO_4$ is also slightly crannied. The $CaMoO_4$:Yb, Er nanocrystals might be anchored on the surface of heparin structure, and then both are interlaced with each other. Finally, approximately spherical biocomposites are obtained.

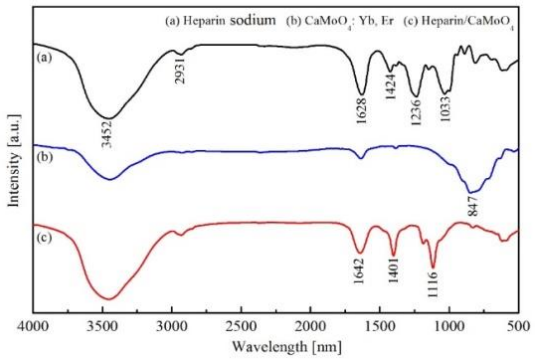

Fig 3. FT-IR spectra of as-prepared $CaMoO_4$:Yb,Er nanocrystals, heparin/$CaMoO_4$ biocomposites, and heparin sodium

Further evidence for the information on the chemical characteristics and surface structure of heparin/$CaMoO_4$ biocomposites was obtained by FT-IR analysis. As shown in Fig 3, two strong peaks at 3452 cm^{-1} and 1628 cm^{-1} are assigned to the strong hydroxyl vibration from H_2O in heparin and the amino group (−NH_2). And other four peaks at 2931 cm^{-1}, 1424 cm^{-1}, 1236 cm^{-1}, and 1033 cm^{-1} are from the stretching vibration of C–H, the deformation vibration of –CH_3, asymmetrical stretching vibration of S=O and the symmetrical stretching vibration of –SO_3, respectively.[13] For $CaMoO_4$:Yb,Er nanocrystals, it is clear that the strong peak at 3460 cm^{-1} (ν_{O-H}) comes from the water molecules adsorbed on $CaMoO_4$:Yb,Er nanocrystals and the peak at 847 cm^{-1} represents the typical Mo–O anti-symmetric stretching vibrations in the $[XO_4]^{2-}$ tetrahedron groups.[14] However, for obtained heparin/$CaMoO_4$ biocomposites, the weakened peak at 1642 cm^{-1} and the enhanced peak at 1401 cm^{-1} and 1116 cm^{-1} imply the coordination interaction between the heparin net structure and the Na_2EDTA chelated $CaMoO_4$:Yb,Er nanocrystals, while the disappearance of the 847 cm^{-1} peak further proves that the the $CaMoO_4$:Yb, Er nanocrystals are anchored on the surface of heparin net structure in the spherical biocomposites.

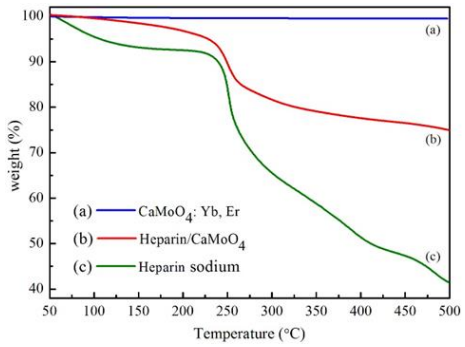

Fig 4. TGA curves of as-prepared $CaMoO_4$:Yb,Er nanocrystals, heparin/$CaMoO_4$ biocomposites, and heparin sodium

The composition changing and different components of $CaMoO_4$:Yb,Er nanocrystals, heparin/$CaMoO_4$ biocomposites, and heparin sodium are investigated by TGA analysis. As shown in Fig 4, TGA trace of $CaMoO_4$:Yb,Er nanocrystals shows little weight loss, which is about 1.2% below 500 °C. Comparing with the $CaMoO_4$:Yb,Er, heparin sodium shows much lower thermal stability. The first one, at range from 50 to 125 °C, is attributed to the evaporation of water. Heparin presents in its structure groups such as carboxylate (–COO−) and sulfonate (–OSO_3−), which are highly hydrophilic and could strongly interact with water molecules through dipole–dipole or ion–dipole forces.[15] The main mass loss takes place around 200−400 °C and is ascribed to the decomposition of labile oxygen functional groups present in the material. There is also a steady mass loss (~8%) over the whole temperature range between 400 and 500 °C, which can be assigned to the removal of more stable oxygen functionalities.[16] And the overall mass loss of heparin is 56%. The TGA curves of heparin/$CaMoO_4$ biocomposites is similar to heparin. The measurement of the sample mass below 500 °C showed that the overall mass loss of heparin/$CaMoO_4$ biocomposites is 25%. It is suggested that the incorporation of $CaMoO_4$ nanoparticles into the biocomposites is about 45%. Furthermore, absent mass loss of heparin/$CaMoO_4$ biocomposites between 400 and 500 °C may be due to that $CaMoO_4$ nanoparticles into the biocomposites prevent the removal of stable oxygen functionalities.

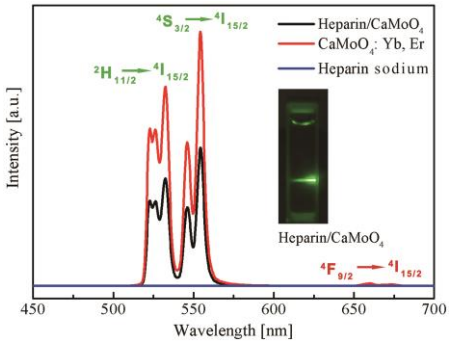

Fig 5. Photoluminescence spectra of $CaMoO_4$:Yb,Er nanocrystals, heparin/$CaMoO_4$ biocomposites, and heparin sodium

Under the 980 nm laser excitation, there is no UC luminescence for the pure heparin sodium. However, the $CaMoO_4$:Yb,Er nanocrystals emit brighter green luminescence than heparin/$CaMoO_4$ biocomposites. As depicted in Fig 5, in the wavelength region of 450-700 nm, the three emission peaks of the as-prepared nanocrystals at 517, 536, and 651 nm are assigned to the $^4H_{11/2}$ to $^4I_{15/2}$, $^4S_{3/2}$ to $^4I_{15/2}$, and $^4F_{9/2}$ to $^4I_{15/2}$ transitions of Er^{3+}, respectively. Under 980 nm excitation, Er^{3+} absorbs one photon and its groundstate ($^4I_{15/2}$) electron is excited to the $^4I_{11/2}$ level. A second photon promotes the electron to the $^4F_{7/2}$ level. The excited electron decays first nonradiatively to $^2H_{11/2}$, $^4S_{3/2}$, and $^4F_{9/2}$ levels. When it decays further to the ground state, UC emission occurs.[17] As shown in the inset of Fig 5, under excitation at 980 nm in a power density only about 50 $mWcm^{-2}$, heparin/$CaMoO_4$ biocomposites dispersed in water show strong green UC luminescence.

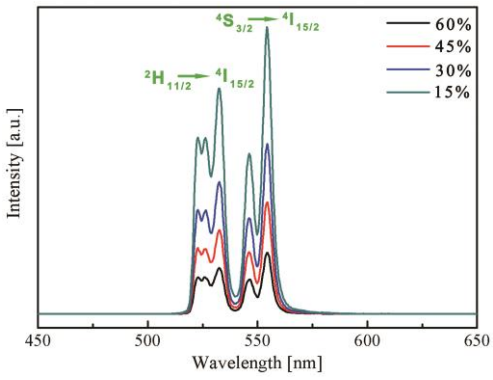

Fig. 6. Photoluminescence spectra of heparin/$CaMoO_4$ biocomposites prepared with different amount of heparin sodium

The PL spectra of heparin/$CaMoO_4$ biocomposites prepared with different amount of heparin sodium are shown in Fig. 6. With the increase of the ratio of heparin sodium, the UC luminescence intensity of heparin/$CaMoO_4$ biocomposites begins to decrease. This may be due to that heparin sodium into heparin/$CaMoO_4$ biocomposites could decrease the UC luminescence intensity of biocomposites. Hence, in the following paragraph, the possible electronic transmissions behavior of photoinduced electron in heparin/$CaMoO_4$ biocomposites is discussed in detail.

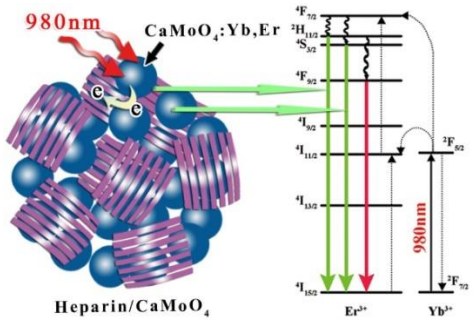

Fig 7. Schematic of the possible photo-induced electron transfer mechanism in heparin/$CaMoO_4$ biocomposites

As illustrated in Fig 7, the $CaMoO_4$:Yb,Er nanocrystals are anchored on the net structure of heparin by chemical bonding, the close distance enables efficient energy transfer from $CaMoO_4$:Yb,Er nanocrystals to the energy receptor in heparin substrate.[17] The electrons in Yb^{3+} are first excited, and then the energy transferred to Er^{3+} further induces the electron excitation, as well as other multiphoton processes in Er^{3+}. The hexamylose or octamylose skeleton, the oxygen-containing functional group, and sulfite containing functional group of heparin/$CaMoO_4$ biocomposites are high-efficiency energy acceptors.[18] So Er^{3+} transfers a fraction of energy to the nearby heparin via the fluorescence resonance energy transfer (FRET) or charge transfer (CT) process instead of the normal nonradiative relaxation of $^2H_{11/2}$ to $^4I_{15/2}$, $^4S_{3/2}$ to $^4I_{15/2}$, and $^4F_{9/2}$ to $^4I_{15/2}$.[19] Therefore, with the increase of heparin sodium, energy transfer and luminescence quenching may enhance, so the UC luminescence of heparin/$CaMoO_4$ biocomposites is weaker.

4. Conclusion

In the present work, green-emitting heparin/$CaMoO_4$ biocomposites are successfully fabricated by a facile hydrothermal method with Na_2EDTA as a chelating agent. And the structure, morphology and fluorescence properties of the heparin/$CaMoO_4$ biocomposites are studied. Obtained heparin/$CaMoO_4$ biocomposites are microsphere with a mean diameter of approximately 150 nm. Heparin into heparin/$CaMoO_4$ biocomposites could decrease the UC luminescence intensity of biocomposites. However, the dispersion of heparin/$CaMoO_4$ shows bright green luminescence under excitation at 980 nm in a power density only about 50 $mWcm^{-2}$.

Acknowledgements

This work was supported by the Innovative Project of Hainan Province in 2015, and the Practice & Innovation Projects of Hainan University in 2016 for financial support. The Instrumental Analysis Centre of Hainan University is also acknowledged here.

References

[1] Y. K. Liang, KL. Kiick, Acta Biomaterialia **10**, 1588 (2014).
[2] S. Ma, Y. Chen, F. Jie, J. Liu, X. Zuo, X. Chen, Analytical Chemistry **88**, 10474 (2016).
[3] TY. Liu, LY. Huang, SH. Hu, MC. Yang, SY. Chen, J Biomed Nanotechnol **3**, 353 (2007).
[4] N. Bogdan, E. M. Rodríguez, F. Sanzrodríguez, et al. **4**, 3647 (2012).
[5] Y. Liu, D. Tu, H. Zhu, X. Chen, Chemical Society reviews **42**, 6924 (2013).

[6] M Haase, H Schäfer, Angewandte Chemie International Edition **50**, 5808(2011).
[7] H. N. Luitel, R. Chand, T. Torikai, M. Yada, T. Watari Rsc Adv **5**, 17034 (2015).
[8] A. Gnach, T. Lipinski, A. Bednarkiewicz, J. Rybka, JA. Capobianco, Chemical Society reviews **44**, 1561 (2015).
[9] F. Wang, X. G. Liu, Chemical Society reviews **38**, 976 (2009).
[10] X. Fernandez-Busquets, Future Med Chem **5**, 737 (2013).
[11] J. Liu, K. Liu, H. Gao, Y. Liu, C. Yang, Z. Liu, J Mater Sci-Mater El **26**, 3380 (2015).
[12] D. M. Zhao, Y. X. Wang, Z. Y. Chen, RW. Xu, G. Wu, DS. Yu, Biomedical materials **3**, 025016 (2008).
[13] G. V. Kumar, CH. Su, P. Velusamy, Materials Letters **180**, 119 (2016).
[14] T. Thongtem, S. Kungwankunakorn, B. Kuntalue, A. Phuruangrat, S. Thongtem, J Alloy Compd **506**, 475 (2010).
[15] M. Baican, E. Paslaru, EG. Hitruc, C. Vasile, Dig J Nanomater Bios **6**, 1053 (2011).
[16] M. M. Sk, C. Y. Yue, RK. Jena Rsc Adv **4**, 5188 (2014).
[17] C. Q. Yang, J. Liu, L. Y. Ma, A. J. Li, Z. X. Liu, Materials Research Bulletin **84,** 283 (2016).
[18] C. Q. Yang, L. Y. N. Ma, SN Wu, et al. J. Mater Sci-Mater El **27**, 11720 (2016).
[19] W. Wei, T He, X Teng, et al. Small **8**, 2271 (2012).